

RSC Medicinal Chemistry

Accepted Manuscript

This article can be cited before page numbers have been issued, to do this please use: G. Leonidis, M. Spathakis, T. Giannakouros, V. Sarli, E. Nikolakaki, G. Kolios and I. Sigala, *RSC Med. Chem.*, 2025, DOI: 10.1039/D5MD00731C.



This is an Accepted Manuscript, which has been through the Royal Society of Chemistry peer review process and has been accepted for publication.

Accepted Manuscripts are published online shortly after acceptance, before technical editing, formatting and proof reading. Using this free service, authors can make their results available to the community, in citable form, before we publish the edited article. We will replace this Accepted Manuscript with the edited and formatted Advance Article as soon as it is available.

You can find more information about Accepted Manuscripts in the <u>Information for Authors</u>.

Please note that technical editing may introduce minor changes to the text and/or graphics, which may alter content. The journal's standard <u>Terms & Conditions</u> and the <u>Ethical guidelines</u> still apply. In no event shall the Royal Society of Chemistry be held responsible for any errors or omissions in this Accepted Manuscript or any consequences arising from the use of any information it contains.



View Article Online

View Journal

Research article

View Article Online
DOI: 10.1039/D5MD00731C

Synthesis of Novel SRPK1-Targeting Hybrid Compounds Incorporating Antimetabolites for Cancer Therapy

George Leonidis,^{a,*} Ioanna Sigala,^a Michail Spathakis,^b George Kolios,^b Thomas Giannakouros,^a Eleni Nikolakaki,^{a,*} and Vasiliki Sarli^{a,*}

- ^a Department of Chemistry, Aristotle University of Thessaloniki, sarli@chem.auth.gr.
- ^b Department of Medicine, Democritus University of Thrace.
- * Author to whom correspondence should be addressed.

Abstract

Serine/arginine protein kinase 1 (SRPK1) plays a pivotal role in the phosphorylation of SR/RS domain-containing proteins, which are involved in various cellular processes. Its overexpression has been associated with the progression of various malignancies, positioning SRPK1 as a promising target for cancer treatment. In this study, we report the design, synthesis, and preliminary biological evaluation of two hybrid molecules, geo15 and geo140, which combine known SRPK1 inhibitors with the antimetabolites gemcitabine and 5-fluorouracil (5-FU), respectively. These conjugates were synthesized to assess whether hybridization enhances potency compared to the parent compounds, and to investigate potential novel mechanisms of action. In vitro assays were performed to evaluate SRPK1 inhibition and antiproliferative activity in selected cancer cell lines. Among the tested compounds, the JH-VII-139-1-based hybrid **geo140** exhibited notable SRPK1 inhibitory potency and cytotoxic effects, demonstrating a favorable profile for further optimization. Interestingly, treatment with geo140 did not appear to alter the overall SRPK1 distribution in interphase cells but resulted in a notable increase of mitotic cells that displayed a substantial accumulation of SRPK1, thus suggesting that the hybrid compound may have an impact on cell cycle progression. This work supports the potential of molecular hybridization as a strategy for the development of novel SRPK1-targeting anticancer agents.

Introduction

Serine/arginine protein kinase 1 (SRPK1) is widely known as a splice factor kinase due to its decisive involvement in the regulation of various steps of mRNA splicing via the phosphorylation of SR splicing factors.¹ However, as the mammalian genome encodes for more than 100 serine-arginine rich proteins -half of which are unrelated to mRNA processing-, the kinase was also shown to regulate diverse cellular activities.²,³ These fundamentally important functions render SRPK1 essential for viability of proliferating cells. Many reports suggest that there is a correlation between SRPK1 overexpression and higher tumor staging, grading, metastasis and shorter survival.⁴,⁵ Consequently, targeting SRPK1 has emerged as a promising therapeutic strategy. Indeed, downregulation of SRPK1 in cancer cells that exhibit high SRPK1 levels suppressed their growth and affected diverse processes heterogeneously, depending on the

oncogenic context.^{4,5,6} For example, vascular endothelial growth factor A (VEGE A) online can produce both proangiogenic and antiangiogenic isoforms; thus, a shift in the splicing machinery towards the production of the former, via upregulation of SRPK1, enhanced angiogenesis.^{7,8} Wang et al. also proposed that aberrant SRPK1 expression induced constitutive Akt activation, thus implying that SRPK1 can mediate tumorigenesis independently of its splicing effects, by modulating signaling pathways such as Akt.⁹ In addition, targeting SRPK1 resulted in enhanced sensitivity to platinumbased chemotherapy in some types of cancer.^{2,4} A wide range of SRPK1 inhibitors have been developed, including SRPIN340, SPHINX, and the more recent JH-VII series compounds, all of which demonstrate potent inhibitory activity against SRPK1.^{4,10,11,12} The growing number of small-molecule inhibitors underlines the pharmacological relevance of SRPK1 as a cancer treatment target.

RSC Medicinal Chemistry

Antimetabolites such as 5-fluorouracil (5-FU) and gemcitabine are cornerstone chemotherapeutic agents used in the treatment of a wide range of solid tumours and hematologic malignancies. These drugs interfere with nucleotide metabolism and DNA synthesis, leading to cell cycle arrest and apoptosis in rapidly dividing cells. Despite their efficacy, limitations such as systemic toxicity, resistance development, and off-target effects often reduce therapeutic outcomes. To overcome these issues, there is growing interest in conjugation strategies that combine antimetabolites with targeting moieties or other pharmacophores to enhance selectivity and synergistic activity.

In previous studies, our group developed peptide-drug conjugates incorporating the oligopeptide c(RGDyK), an integrin $\alpha_{\nu}\beta_{3}$ ligand, for the targeted delivery of SRPK1 inhibitors (SRPIN803, JH-VII-139-1). 13,14,15,16 These studies yielded promising results, demonstrating both the synergistic effects of the two pharmacophores and novel applications. As a following step, we sought to explore the concept of molecular hybridization by covalently linking SRPK1 inhibitors with antimetabolites, inspired by previous research showing that targeting of SRPK1 results in enhanced sensitivity to platinum-based drugs in some types of cancer.^{2,4} Our aim was to evaluate whether these hybrids could exhibit enhanced potency, improved physicochemical properties, or new mechanisms of action compared to the parent pharmacophores. Specifically, SRPIN803 was coupled with gemcitabine, and JH-VII-139-1 with 5-fluorouracil, producing the hybrid compounds geo15 and geo140, respectively (Figure 1). Herein, we describe the synthesis of these hybrids and evaluate their chemostability in buffer media, DMEM, and human plasma. Additionally, we report on their biological properties, including cellular viability, SRPK1 inhibition, subcellular distribution of the kinase, and a potential mode of action of geo140.

View Article Online DOI: 10.1039/D5MD00731C

Figure 1. Structures of novel SRPK1-targeting hybrids that incorporate antimetabolites

Synthesis of SRPK1-targeting hybrids

Synthesis of conjugate geo15

Based on our prior experience synthesizing two SRPIN803-c(RGDyK) conjugates bearing non-cleavable ether and secondary carbamate linkers, our next goal was to design a linker with sufficient stability for attachment to the phenolic group of **SRPIN803** without being readily hydrolyzed. We selected *para*-aminobenzyl alcohol (3), which is converted to para-aminobenzyl ether (PABE, 1) upon coupling with phenol and carboxylic acid derivatives. PABE is a cleavable linker capable of self-immolation via a 1,6-elimination mechanism following hydrolysis at the aniline end (Figure 2). Recent literature shows that PABE linkers are used in various hybrid drugs containing phenolic ends, which are often susceptible to hydrolysis.

Figure 2. Self-immolation mechanism of PABE linkers

To facilitate the coupling reactions of the PABE linker, a glycine moiety to the aniline side was attached through an amidation reaction, introducing a more reactive primary amine that does not interfere with the self-immolation mechanism. The synthetic route started with the preparation of bocylated glycine 4 from commercially available glycine, which reacted with Boc₂O under basic conditions to yield the desired product with 43% yield (Scheme 1). Before the amidation step, compound 4 was activated with *N*-hydroxysuccinimide and DCC, producing the isolable activated ester 5 in 60% yield.

Ester **5** and *para*-aminobenzyl alcohol then readily reacted to form the desired producted Article Online **6** in 71% yield. Compound **6** was subsequently treated with phosphorus tribromide in diethyl ether, resulting in the unstable bromide intermediate **7** in 45% yield. Bromide **7** was then immediately reacted with SRPIN803 in a Williamson ether synthesis, yielding the intermediate **8** with a 46% yield. The synthetic route ended with Boc deprotection under acidic conditions, isolating the SRPIN803 derivative **9** as a TFA salt in 47% yield.

Scheme 1. Synthetic route of SRPIN803 derivative 9

With the TFA salt of primary amine **9** in hand, we proceeded with a coupling reaction with the activated gemcitabine **10**, yielding the Boc-protected SRPIN803-gem conjugate **11** in 67% yield (Scheme 2). As reported in our previous work, activated gemcitabine **10** was obtained through consecutive protection and activation reactions of gemcitabine hydrochloride. ¹⁹ The final desired conjugate **geo15**, was obtained after deprotection of the two Boc groups on gemcitabine using a solution of TFA in DCM. Conjugate **geo15** was isolated by HPLC as a yellow, fluorescent solid with purity over 99% and yield 90%. The calculated exact mass for the [M+H]⁺ ion of the final conjugate is 822.1724, and a mass of 822.0 was observed in the mass spectrometer.

Scheme 2. Synthesis of conjugate geo15 and its LC-MS elution chromatogram. Method: 3.

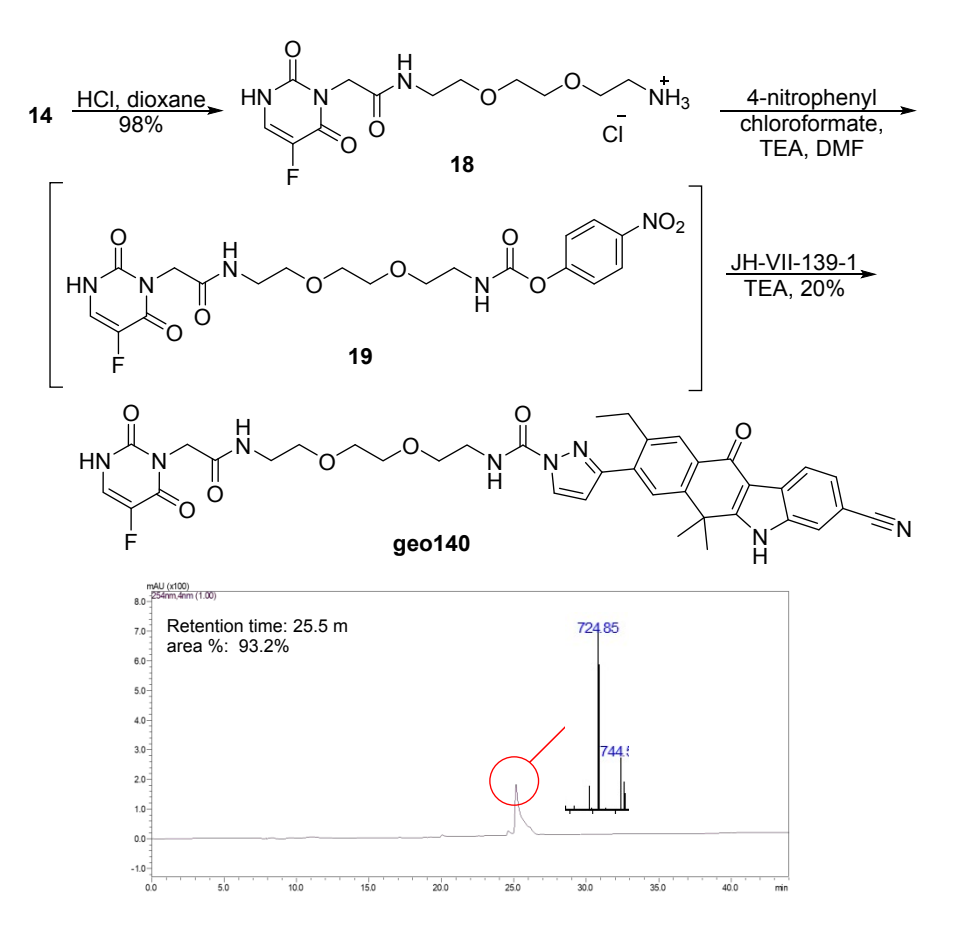
Synthesis of conjugate geo140

The synthesis of the hybrid compound of JH-VII-139-1 with 5-FU, **geo140** started with the preparation of the carboxylic acid derivative of the antimetabolite 5-FU, compound **12**. As reported in our previous work, 5-FU was alkylated with bromoacetic acid under basic conditions to yield derivative **12** in 82% yield. Compound **12** was then reacted with the Boc-protected amine **13** in the presence of HOBt, EDCI, and TEA, resulting in the formation of the desired amide **14** in 76% yield (Scheme 3). Compound **14** was deprotected with TFA in DCM, yielding the TFA salt **15** in near-quantitative conversion. In the next step, activation with 4-nitrophenyl chloroformate did not afford the desired activated ester **16**, but instead exclusively gave the undesired amide **17**. A possible explanation for this result is the nucleophilic attack on the activated ester **16** by trifluoroacetate ions. Despite their weak nucleophilicity, trifluoroacetate ions can react with the highly electrophilic **16** in the presence of a base.

The problem was resolved by changing the deprotection conditions of **14**. After adding a hydrochloric acid solution in dioxane, the deprotected hydrochloride salt **18** was obtained with a 98% yield (Scheme 4). Activation with 4-nitrophenyl chloroformate ester proceeded easily to the 4-nitrophenyl carbamate **19**. Due to its instability, ester **19** was not isolated, and its solution was used in the subsequent step. Finally, the activated ester **19** reacted with the inhibitor JH-VII-139-1 in an amidation reaction in the presence of triethylamine, affording the desired conjugate **geo140** in 20% yield. Although quite polar, **geo140** was isolated as a green, fluorescent solid after column

chromatography with a purity of 93%. The final conjugate has a calculated exact mass of 724.85 was detected in the mass spectrometer.

Scheme 3. Attempted synthesis of activated ester 16.



Scheme 4. Synthesis of the conjugate geo140 and its LC-MS chromatogram. Method: 1

In Vitro Stability Studies

View Article Online DOI: 10.1039/D5MD00731C

The stability of SRPK1-targeting conjugates **geo15** and **geo140** was assessed at pH 5.2 and 7.4, as well as in cell culture medium (DMEM) and human plasma. All experiments were conducted at 37 °C, with samples analysed by LC-ESI-MS at specific time points. **Geo140** demonstrated high stability across all tested conditions, as shown in Figure 4 (and Supplementary Figures S16 and S17). In contrast, **geo15** displayed varying stability profiles, with *retro*-Knoevenagel degradation and the release of **21** being the primary reaction observed. The half-lives of the conjugates ranged from several minutes to several hours, is discussed below.

Chemostability profile of geo15

The relative percentage concentration of **geo15** over time is presented, measured at incubation times from t=0 to t=48 (Figure 3). Similar to the stability of the peptide conjugates of SRPIN803 (**geo41** and **geo35**) published in our previous work, ¹⁵ the hybrid **geo15** was less stable in the pH 5.2 buffer (with a half-life of 23 hours and 55 minutes) compared to pH 7.4, DMEM and plasma buffers (half-life greater than 48 hours)(Figure 3). Nevertheless, the overall stability profile was suitable for further studies, as the concentration of the conjugate remained above 50% during the 24-hour period.

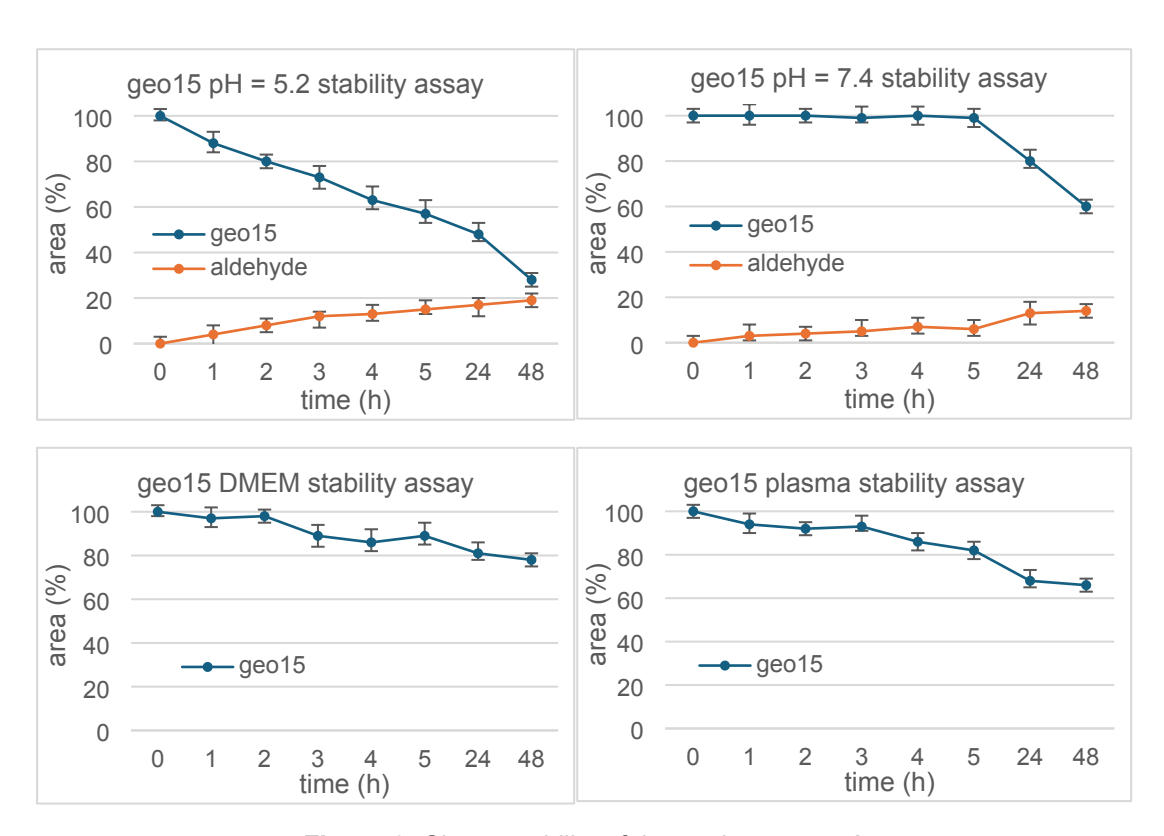


Figure 3. Chemostability of the conjugate geo15

A small percentage of the *retro*-Knoevenagel reaction product **21** (Scheme 5) was also possible or detected in the pH buffer media. However, it was not observed in the DMEM or plasma media, where the conjugate exhibited overall greater stability. Finally, no release of SRPIN803 via the 1,6-elimination mechanism was observed. For 1,6-elimination to occur, hydrolysis of the amide bond must first take place, a reaction that may take place inside the cell.

Scheme 5. Retro-Knoevenagel Reaction of geo15

Chemostability profile of geo140

The conjugate **geo140** demonstrated great stability in both buffer media, with half-lives exceeding 48 hours. It also remained stable in DMEM and human plasma, although a 10–20% reduction in its initial concentration was observed after 24 hours (Figure 4). This profile was attributed to the presence of chemically stable amide and urea anchor points.

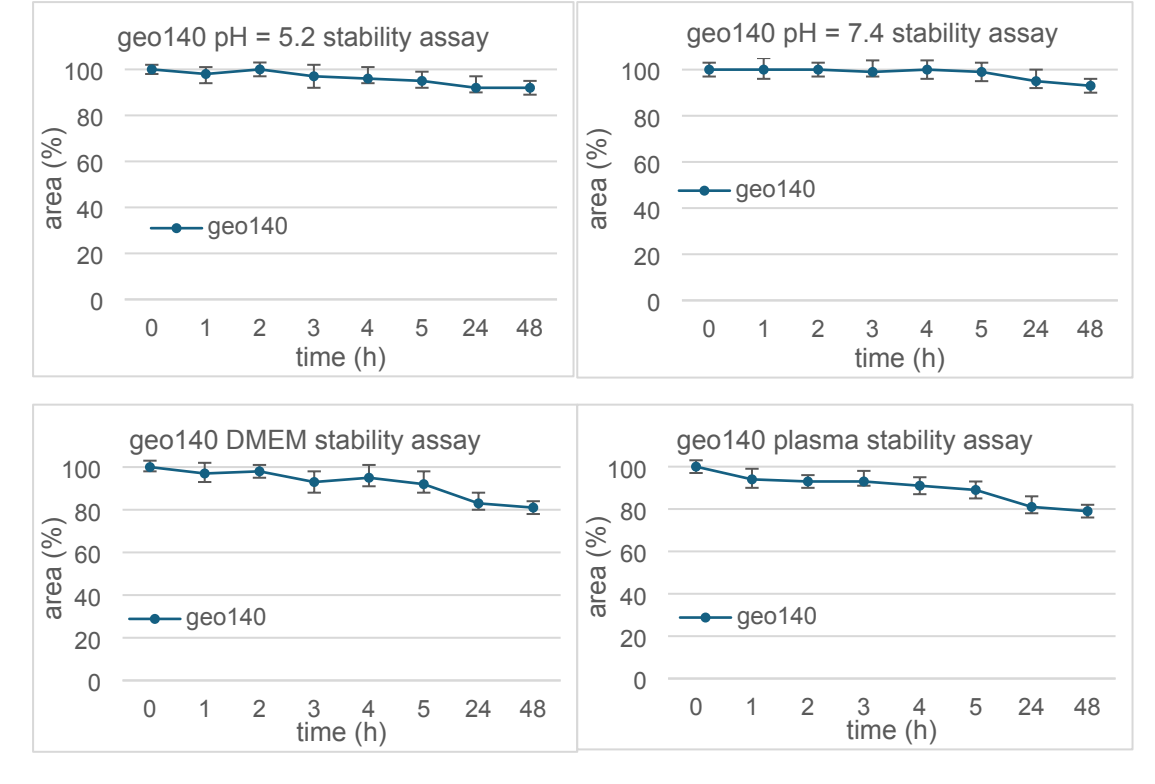


Figure 4. Chemostability of conjugate geo140

Biological Activity of the Synthesized Compounds

View Article Online DOI: 10.1039/D5MD00731C

Cytotoxicity of the hybrid compounds geo15 and geo140

To evaluate the cytotoxic effects of the hybrid compounds **geo15** and **geo140**, we performed MTT assays on HeLa, K562, A549, HepG2, HT-29 and Caco2 cancer cell lines, as well as primary intestinal subepithelial myofibroblasts (SEMFs). The half-maximal effective concentration (EC $_{50}$) values were determined after 48 hours of treatment and are presented in Tables 1 and 2.

Geo140, the hybrid compound of 5-FU with JH-VII-139-1, exhibited significant cytotoxic activity across all cell lines tested, apart from A549 cells. The EC $_{50}$ values for **geo140** for every cell line are listed in Table 1. In all cell lines tested **geo140** cytotoxic effect was less potent than its parent compound JH-VII-139-1, with HeLa and K562 being the most sensitive cell lines.

Table 1. Half maximal effective concentrations (EC₅₀ values) of **5-FU**, **JH-VII-139-1** and **geo140**, in cancer cell lines HeLa, K562, A549, HepG2, HT-29, Caco2 and SEMFs following treatment for 48h. Data represent the mean of three independent experiments.

	EC ₅₀ (µM)									
	HeLa	K562	A549	HepG2	HT-29	Caco2	SEMFs			
5-FU	25.7	>50	15.19	>50	3.62	>50	>50			
JH-VII-139-1	8.6	13.2	>50	16.66	1.4	14.77	12.84			
geo140	11.7	13.7	>50	27.14	19.33	31.24	21.5			

Table 2. Half maximal effective concentrations (EC₅₀ values) of gemcitabine, **SRPIN803** and **geo15**, in cancer cell lines HeLa, K562, A549, HepG2, HT-29, Caco2 and SEMFs following treatment for 48h. The data represent the mean of three independent experiments.

	EC ₅₀ (µM)									
	HeLa	K562	A549	HepG2	HT-29	Caco2	SEMFs			
Gemcitabine	6.7	>50	>50	31.44	28.67	>50	>50			
SRPIN803	60.1	>50	14.45	32.51	>50	31.64	>50			
geo15	33.1	>50	>50	>50	38.36	>50	>50			

Geo15, the hybrid of gemcitabine and SRPIN803, presented reduced cytotoxicity in all cell lines tested as compared to its parent compounds, except for HeLa and HT-29 cells, in which **geo15** was more potent than SRPIN803.

Given the limited cytotoxicity of **geo15** and its lack of efficacy in K562, A549, HepG2, Caco2 cells and primary SEMFs, we decided not to extend its biological evaluation further and continued our studies with **geo140** which demonstrated a more consistent cytotoxic effect towards almost all the tested cell lines.

Inhibition of SRPK1 and SRPK2 kinase activity by **JH-VII-139-1** and the hybridew Article Online compound **geo140**

The inhibitory activity of **geo140** and JH-VII-139-1 against SRPK1 and SRPK2 was assessed using *in vitro* kinase assays (Figure 5). **Geo140** inhibited the activity of SRPK1 and SRPK2 toward LBRNt(62–92), a well-known substrate of the kinase²⁰ with IC₅₀ values of 22.1 nM and 7.9 μ M, respectively, comparable with the respective IC₅₀ values obtained with JH-VII-139-1 alone (Figure 5E). The IC₅₀ values summarized in Panel E indicate that both JH-VII-139-1 and the hybrid compound **geo140** act as effective inhibitors of SRPK-mediated phosphorylation, with however, differential selectivity between SRPK1 and SRPK2.

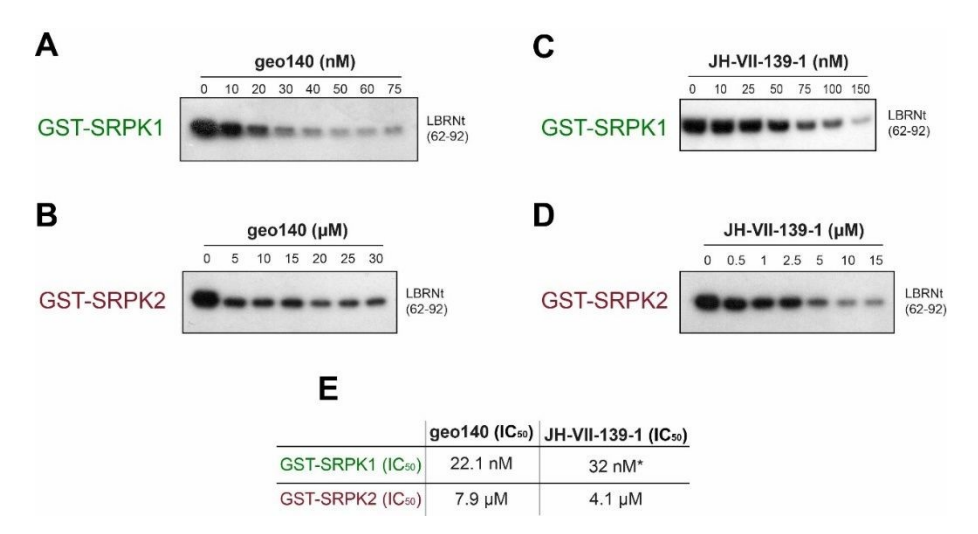


Figure 5. Phosphorylation of 1 μg GST-LBRNt(62–92) by 0.5 μg GST-SRPK1 or 0.5 μg GST-SRPK2 in the presence of increasing concentrations of **geo140** (A and B, respectively) or in the presence of increasing concentrations of JH-VII-139-1 (C and D, respectively). Panel C was taken from a previous publication of the authors. 2 The samples were analyzed by SDS-PAGE on 12% gels, stained with Coomassie Blue and autoradiographed. Only the relevant part of the autorad corresponding to the phosphorylated substrate is shown. E. IC₅₀ values of **geo140** and JH-VII-139-1 against GST-SRPK1 and GST-SRPK2.

Effect of geo140 on the subcellular localization of SRPK1

In a following step the effect of **geo140** was tested on the subcellular distribution of SRPK1 in HeLa cells. To address this issue, a series of immunofluorescence experiments was performed to assess the effect of **geo140**, relative to its parent compounds, JH-VII-139-1 and 5-FU on SRPK1 localization.

In control cells, SRPK1 predominantly localized to cytoplasm, while treatment with JH-VII-139-1 (20 μ M, 24 h) did not affect the cytoplasmic localization of the kinase (Figure 6). Exposure of cells to 20 μ M 5-FU for 24 h, led to a more diffuse SRPK1 staining pattern, with some nuclear translocation of the kinase, while treatment of cells with 5-FU, for 48 h, resulted in almost complete nuclear translocation of SRPK1, corroborating previous reports showing the induction of SRPKs' nuclear translocation in response to stress and especially chemotherapeutic agents. ^{21,22,23,24} As the kinase

activity is essential for the entry of SRPKs into the nucleus, addition of the inhibitor JHView Article Online VII-139-1, prevented the nuclear accumulation of SRPK1 in 5-FU-treated cells, in accordance with previous observations.¹⁶

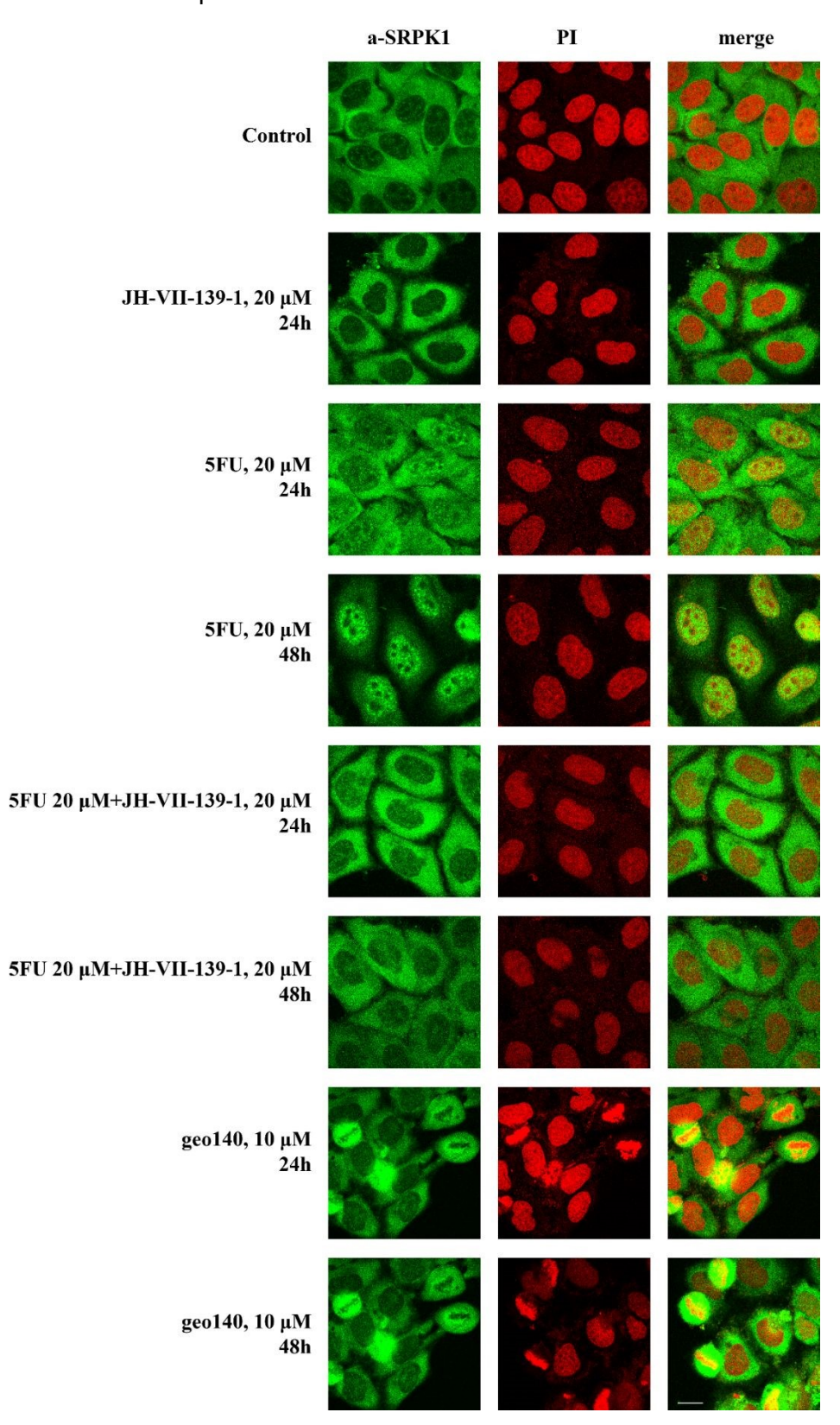


Figure 6. Fluorescent patterns of SRPK1 in HeLa cells treated with JH-VII-139-1, 5-FU, and **geo140** (for the indicated concentrations and time periods). SRPK1 was detected using an anti-

SRPK1 monoclonal antibody (Alexa488-green fluorescence) while nuclei were stained with Plew Article Online DOI: 10.1039/D5MD00731C (red fluorescence). Scale bar: 10 µm.

Interestingly, addition of the newly synthesized hybrid compound, **geo140** resulted in a different pattern than that observed with co-treatment of cells with JH-VII-139-1 and 5-FU. While in interphase cells SRPK1 retained a cytoplasmic distribution similar to that seen in untreated controls, a significant increase in the number of mitotic cells was observed. In these cells, SRPK1 was not associated but rather surrounded by condensed chromosomes.

A similar morphology of **geo140**-treated cells was also observed using an inverted phase-contrast microscope. As shown in Figure 7, a significant increase in mitotic cells, characterized by their round shape and distinct chromosomal structures, was observed.

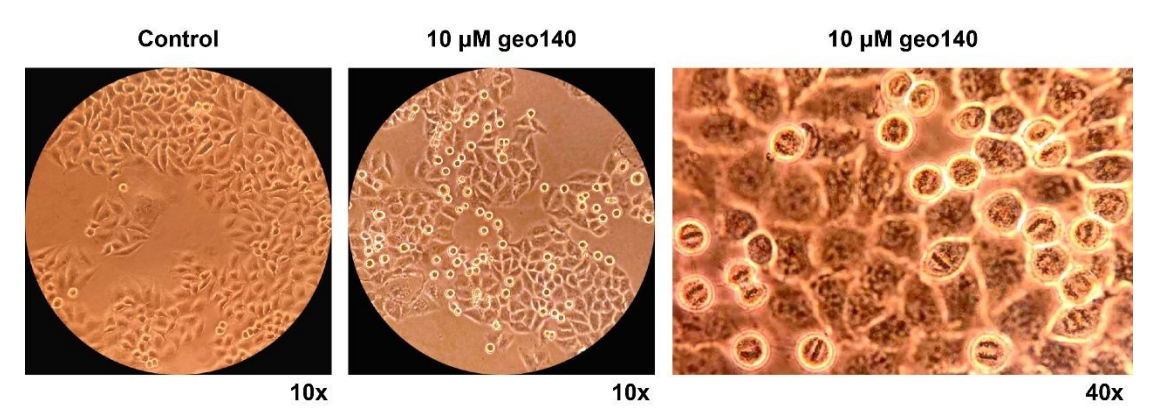


Figure 7. Microscopic view of control Hela cells and treated with 10 μM **geo140**, taken at 10x or 40x magnification as indicated, using an inverted phase-contrast microscope.

These observations suggest that a significant number of HeLa cells are unable to exit mitosis upon treatment with **geo140**. Further studies are required to clarify the mechanism of **geo140** imposing a mitotic arrest and the potential involvement of SRPK1 on it.

Conclusion

In this work, we aimed to develop dual-targeting conjugates capable of simultaneously inhibiting the SRPK1 kinase while incorporating antimetabolite functionality to achieve synergistic anticancer effects. Building on the experiences gained from our work with peptide drug conjugates, we were inspired by previous studies showing that targeting of SRPK1 results in enhanced sensitivity to platinum-based chemotherapy in some types of cancer.^{2,4} Two hybrid molecules, geo15 and geo140, were designed and synthesized which combine known SRPK1 inhibitors (SRPIN803, JH-VII-139-1) with the antimetabolites gemcitabine and 5-FU. The hybrid of 5-FU with JH-VII-139-1, geo140, exhibited significant cytotoxic activity comparable to JH-VII-139-1 across all cell lines tested except A549. On the other hand, the hybrid of gemcitabine with SRPIN803, geo15, presented reduced cytotoxicity in all cell lines tested as compared to its parent compounds, except for HeLa and HT-29 cells, in which geo15 was more potent than SRPIN803. The conjugate geo140 preserved the activity of the parent compound JH-VII-139-1 against SRPK1 and SRPK2 with IC₅₀ values of 22.1 nM and 7.9 µM, respectively. Therefore, we noticed that the antiproliferative efficacy of the conjugates **geo140** and **geo15** was correlated with the activity of the SRPK1 inhibitor.

JH-VII-139-1 is a stable and nanomolar SRPK1 inhibitor, whereas SRPIN803 is Jew Article Online micromolar inhibitor. Although 5-FU exhibits lower cytotoxicity than gemcitabine, its conjugation with JH-VII-139-1 yielded a hybrid compound with enhanced cytotoxic potency particularly against HeLa and K562 cells. When examining the effect of geo140 on the subcellular localization of SRPK1 we found that the conjugate geo140 resulted in a different phenotype than that observed with co-treatment of cells with JH-VII-139-1 and 5-FU. Our results demonstrate that compound geo140 did not alter the subcellular localization of SRPK1, but had a profound effect on cell cycle regulation. This observation may be explained by a novel mechanism of action of the hybrid, involving the dual activity against SRPK1 and antimetabolite-mediated inhibition of cell growth. Alternatively, geo140 may exert its effects by interfering with a different molecular target. While additional studies are warranted to elucidate the molecular mechanisms underlying these observations, this work supports the potential of molecular hybridization as an innovative approach for the development of novel SRPK1-targeting anticancer agents with potential therapeutic relevance.

Data availability

The data supporting this article are available in its ESI. The ESI contains copies of ¹H and ¹³C NMR spectra, 2D NMR spectra, MS spectra, and analytical HPLC traces for all final compounds.

Author contributions

V.S., E.N. and G. L. conceived the study. G. L. synthesized the compounds. G.L. performed protein mass spectrometry experiments, HPLC analysis and stability studies. I. S. carried out biochemical kinase assays, I. S., G. K., M. S., E.N., T. G. carried out and supervised the cytotoxicity screening, V. S, T.G., E.N. and G. K. acquired funding to carry out the project. G. L., V. S., E. N., T.G. wrote the manuscript, and all authors contributed to manuscript editing.

Conflicts of interest

The other authors declare no competing interests.

Chemistry

All reactions were conducted under an argon atmosphere unless otherwise specified, using commercial reagents without additional purification. Reactions were monitored by thin-layer chromatography (TLC), visualized under UV light, and developed with aqueous ceric sulfate/phosphomolybdic acid, ethanolic *p*-anisaldehyde solution, potassium permanganate solution, and heat. 1 H and 13 C NMR spectra were recorded at 500 MHz and 126 MHz, respectively, on an Agilent spectrometer, with tetramethylsilane (TMS) as an internal standard. Chemical shifts are reported in δ (ppm) from internal reference peaks (TMS 1 H 0.00; CDCl $_{3}$ 1 H 7.26, 13 C 77.16, (CD $_{3}$) $_{2}$ SO 1 H 2.50, 13 C 39.52, (CD $_{3}$) $_{2}$ CO 1 H 2.05, 13 C 29.84, 206.26). LC-MS analysis was performed on a Shimadzu LC-20AD system connected to a Shimadzu LCMS-2010EV (Shimadzu, Kyoto, Japan), equipped with a C₁₈ analytical column (Supelco Discovery C18, 5 µm, 250 × 4.6 mm).

(tert-butoxycarbonyl)glycine, 4: In a solution of glycine (1.00 g, 13.3 mmol) and saturated potassium hydroxide (29 g, 520 mmol) in dioxane and water (40 mL, 1:1),

Boc₂O (3.7 mL, 16.0 mmol) was added. The addition was carried out at room temperature, and the reaction was stirred for 12 hours. After the reaction was complete, the solvent was evaporated, and the residue was dissolved in ethyl acetate. The organic phase was washed with 10% aqueous sodium sulfate and brine. The organic layers were collected, dried over Na_2SO_4 , and concentrated *in vacuo*. The white solid residue **4** (2.33 g, 43%) was used in subsequent reactions without any further purification. The spectroscopic data agree with the literature values.²⁵ **4**: ¹H NMR (500 MHz, CDCl₃) δ 5.04 (s, 1H), 3.96 (s, 2H), 1.45 (s, 9H).

2,5-dioxopyrrolidin-1-yl (tert-butoxycarbonyl)glycinate, **5**: To a solution of Boc-glycine **4** (141 mg, 0.805 mmol) and NHS (140 mg, 1.22 mmol) in dry THF (2 mL), a solution of DCC (327 mg, 1.95 mmol) in dry THF (2 mL) was added. The addition takes place under an argon atmosphere, and the reaction was stirred for 24 hours at room temperature. During the work-up, a few drops of acetic acid were added, and after 1 hour of stirring, the mixture was filtered under vacuum to remove the insoluble DCU. The filtrate was then concentrated, and the resulting residue was dissolved in 2-propanol and stirred at room temperature for 1 hour. The resulting suspension was filtered under vacuum and washed with 2-propanol. Finally, **5** (132 mg, 60%) was obtained as a white solid and used in subsequent reactions without further purification.²⁶ **5**: ¹H NMR (500 MHz, CDCl₃) δ 4.95 (s, 1H), 4.29 (d, J = 5.4 Hz, 2H), 2.85 (s, 4H), 1.46 (s, 9H).

tert-butyl (2-((4-(hydroxymethyl)phenyl)amino)-2-oxoethyl)carbamate, **6**: A solution of Boc-glycine *N*-hydroxysuccinimide ester **5** (110 mg, 0.404 mmol) and para-aminobenzyl alcohol (100 mg, 0.812 mmol) in dry dichloromethane (1.5 mL) was stirred under an argon atmosphere at room temperature for 48 hours. The reaction was concentrated, and the resulting residue was redissolved in dichloromethane and washed with a 0.1N hydrochloric acid solution (0.5 mL) and water (0.5 mL). The organic layers were collected, dried over Na_2SO_4 , and concentrated under vacuum. The solid residue was subjected to column chromatography (petroleum ether / ethyl acetate, gradient elution from 1 / 1 to 1 / 2), and the desired alcohol **6** (80 mg, 71%) was obtained as a brown oil. Spectroscopic data were in agreement with the literature values.^{27 1}H NMR (500 MHz, CDCl₃) δ 8.08 (s, 1H), 7.51 (d, J = 8.3 Hz, 2H), 7.33 (d, J = 8.3 Hz, 2H), 5.17 (s, 1H), 4.66 (s, 2H), 3.92 (d, J = 6.0 Hz, 2H), 1.49 (s, 9H).

tert-butyl (2-((4-(bromomethyl)phenyl)amino)-2-oxoethyl)carbamate, **7**: To a cold (0 °C) solution of **6** (67 mg, 0.239 mmol) in dry dichloromethane (3.3 mL), phosphorus tribromide (7.64 μ L, 0.081 mmol) was added. The addition was made under an argon atmosphere, and the reaction was stirred for 30 minutes at 0 °C. After that, cold water was added to the reaction, followed by extractions with dichloromethane. The organic layers were collected, dried over Na₂SO₄, and concentrated in vacuum. The obtained yellow solid **7** (37 mg, 45%) was used in subsequent reactions without any further purification. **7**: ¹H NMR (500 MHz, CDCl₃) δ 8.14 (s,1H), 7.49 (d, J = 8.5 Hz, 2H), 7.35 (d, J = 8.5 Hz, 2H), 5.17 – 5.11 (m,1H), 4.48 (s, 2H), 3.91 (d, J = 6.1 Hz, 2H), 1.53 (s, 9H).

tert-butyl (E)-(2-((4-((5-(2-cyano-3-oxo-3-((5-(trifluoromethyl)-1,3,4-thiadiazol-2-yl)amino)prop-1-en-1-yl)-2-methoxyphenoxy)methyl)phenyl)amino)-2-oxoethyl)carbamate, **8**: To a solution of **7** (177 mg, 0.516 mmol) and SRPIN803 (210

mg, 0.567 mmol) in dry dimethylformamide (3.83 mL), potassium carbonate ($78.4 \text{ mg}^{\text{dise} \text{Article} \text{Online}}$) 0.567 mmol) were added. The addition was made at room temperature, and the reaction was left stirring for 24 hours at room temperature. The solvent was removed *in vacuo*, and the resulting yellow residue **8** (426 mg, 46%) was used in subsequent reactions without any further purification. **8:** 1 H NMR (500 MHz, DMSO- d_6) δ 10.01 (s, 1H), 7.74 (d, J = 8.5 Hz, 1H), 7.56 – 7.52 (m, 3H), 7.42 (d, J = 8.5 Hz, 1H), 7.38 (d, J = 8.5 Hz, 2H), 7.05 – 7.02 (m, 1H), 5.40 (s, 1H), 4.68 (s, 2H), 3.71 (d, J = 5.9 Hz, 2H), 1.39 (s, 9H), -OCH₃ peak is overlapping with DMSO- d_6 water peak. 13 C NMR (126 MHz, DMSO- d_6) δ 169.1, 168.8, 165.4, 163.9, 156.4, 141.4, 139.4, 138.0, 133.0, 132.8, 130.4, 127.4, 122.3, 120.0, 119.5, 119.2, 117.9, 110.7, 105.2, 78.5, 63.0, 44.2, 35.3, 28.7. ESI-MS, positive mode: m/z calcd mass for $C_{28}H_{27}F_3N_6O_6S$ [M+H]⁺ = 633.1738, was found 633.15.

(E)-3-(3-((4-(2-aminoacetamido)benzyl)oxy)-4-methoxyphenyl)-2-cyano-N-(5-(trifluoromethyl)-1,3,4-thiadiazol-2-yl)acrylamide TFA salt, 9: To a solution of 8 (326 mg, 0.515 mmol) in dry dichloromethane (4.8 mL), a solution of trifluoroacetic acid in dichloromethane (2.4 mL, 31.4 mmol in 2.4 mL) was added dropwise. The addition was made under argon atmosphere, at 0 °C, and the reaction was stirred for 20 minutes at 0 °C. The solvent was removed under vacuum, and the residue was dissolved in NaHCO₃(aq) to adjust the pH to 7. The solution was then extracted with ethyl acetate, the organic layers were collected, dried with Na₂SO₄, and concentrated under vacuum. The resulting residue was subjected to column chromatography (dichloromethane/methanol, gradient elution from 10:1 to 10:2.5) and preparative thinlayer chromatography (dichloromethane/methanol 10:2), to yield the desired compound 9 (128 mg, 47%) as a yellow, fluorescent solid. 9: 1H NMR (500 MHz, DMSO- d_6) δ 8.36 (s, 1H), 7.78 (d, J = 1.8 Hz, 1H), 7.63 (d, J = 8.5 Hz, 2H), 7.59 (dd, J = 9.0, 1.7 Hz, 1H), 7.48 (d, J = 8.5 Hz, 2H), 6.80 (d, J = 8.5 Hz, 1H), 5.63 (s, 2H), 3.80 (s, 3H), 3.48 (s, 2H). 13 C NMR (126 MHz, DMSO- d_6) δ 170.8, 168.9, 164.1, 152.8 (J = 4.2 Hz), 148.6, 144.7 (J = 40.9 Hz), 138.7, 129.6, 129.4, 129.3, 129.2, 128.9,122.4, 121.1, 119.2, 119.1, 119.0, 118.5, 117.1, 113.1, 109.5, 55.4, 54.4, 43.4. ESI-MS, positive mode: m/z calcd mass for $C_{23}H_{19}F_3N_6O_4S$ [M+H]⁺ = 533.1213, was found 533.00.

Boc-protected SRPIN803-gem conjugate, 11: To a solution of compound **9** (5 mg, 0.0105 mmol) and compound **10** (6.61 mg, 0.0105 mmol) in dry dimethylformamide (0.176 mL), dry triethylamine (2.93 μL, 0.021 mmol) was added. The addition was performed under an argon atmosphere, and the reaction was stirred for 2 days at room temperature. The solvent was removed under vacuum, and the resulting residue was subjected to column chromatography (petroleum ether/ethyl acetate, gradient elution from 1:1 to 1:5) to isolate the desired protected conjugate **11** (11 mg, 67%) as a fluorescent yellow solid. ¹H NMR (500 MHz, acetone- d_6) δ 9.35 (s, 1H), 8.51 (s, 1H), 8.04 (d, J = 7.6 Hz, 1H), 7.95 (d, J = 1.9 Hz, 1H), 7.71 – 7.68 (m, 3H), 7.58 (d, J = 8.4 Hz, 2H), 7.32 (d, J = 7.7 Hz, 1H), 7.04 (d, J = 8.3 Hz, 1H), 6.96 (s, 1H), 6.38 (s, 1H), 5.72 – 5.70 (m, 2H), 5.34 – 5.28 (m, 1H), 4.64 (d, J = 12.2 Hz, 1H), 4.48 – 4.43 (m, 1H), 4.39 (dd, J = 12.5, 4.0 Hz, 1H), 4.05 – 3.97 (m, 2H), 3.95 (s, 3H), 1.51 (s, 9H), 1.48 (s, 9H). ¹³C NMR (126 MHz, acetone- d_6) δ 171.6, 168.5, 166.1, 164.6, 157.1, 155.0, 154.4, 153.1, 152.7, 152.5, 146.7, 145.8, 140.2, 130.8, 130.3, 128.6, 125.2, 123.3, 120.4, 119.7, 118.2, 116.6, 114.0, 105.5, 96.1, 84.5, 82.5, 78.3, 73.8, 62.8,

56.4, 55.8, 45.5, 45.3, 28.2, 27.7. ESI-MS, positive mode: m/z calcd mass follow Article Online $C_{43}H_{44}F_5N_9O_{13}S$ [M+H]⁺ = 1022.2772, was found 1021.95.

Conjugate **geo15**: In a cold solution of **11** (3.8 mg, 3.7 μmol) in dry dichloromethane (60 μL), a solution of trifluoroacetic acid (17.4 μL, 0.227 mmol) in dichloromethane (30 μL) was added dropwise. The addition was performed under an argon atmosphere, and the reaction was stirred at 0°C for 30 minutes. The solvent was removed by lyophilization, and the crude residue was subjected to semi-preparative HPLC (method 3) to isolate **geo15** (1.5 mg, 90%) as a fluorescent yellow solid. ¹H NMR (500 MHz, DMSO- d_6) δ 10.07 (s, 1H), 8.47 (s, 1H), 7.83 (s, 1H), 7.70 – 7.64 (m, 2H), 7.60 (d, J = 8.4 Hz, 2H), 7.52 (d, J = 7.5 Hz, 1H), 7.47 (d, J = 8.4 Hz, 2H), 7.43 – 7.35 (m, 2H), 6.94 (d, J = 8.3 Hz, 1H), 6.42 (s, 1H), 6.22 – 6.17 (m, 1H), 5.82 (d, J = 7.5 Hz, 1H), 5.65 (s, 2H), 4.37 (d, J = 11.4 Hz, 1H), 4.24 – 4.17 (m, 2H), 3.96 (s, 1H), 3.84 (s, 3H), 3.82 – 3.79 (m, 2H). ¹³C NMR (126 MHz, DMSO- d_6) δ 170.5, 168.0, 167.7 165.6, 164.7, 156.2, 154.6, 153.6, 150.4, 148.8, 148.1, 145.0, 141.1, 139.0, 129.5, 129.1, 127.8, 122.8, 121.3, 121.1, 119.2, 118.4, 117.8, 116.3, 113.7, 102.4, 95.0, 77.5, 69.8, 62.3, 55.6, 54.5, 44.0. ESI-MS, positive mode: m/z calcd mass for C₃₃H₂₈F₅N₉O₉S [M+H]⁺ = 822.1724, was found 822.0.

(2-(2-(2-(2-(5-fluoro-2,6-dioxo-3,6-dihydropyrimidin-1(2H)-yl)acetamido) tert-butyl ethoxy)ethoxy)ethyl)carbamate. 14: To a solution of carboxylic acid derivative 12 (67 mg, 0.356 mmol) and amine 13 (88.4 mg, 0.356 mmol) in dry dimethylformamide (5 mL), HOBt (72.2 mg, 0.534 mmol), triethylamine (150 μL, 1.07 mmol), and EDCi (102 mg, 0.534 mmol) were added. The additions were performed under an argon atmosphere, and the reaction was stirred for 24 hours at room temperature. After completion, the solvent was removed under vacuum, and the resulting residue was subjected to column chromatography (dichloromethane/methanol, gradient elution from 10/0.3 to 10/1.5) to isolate the desired amide 14 (114 mg, 76%) as a white crystalline solid. ¹H NMR (500 MHz, acetone- d_6) δ 7.82 (d, J = 6.5 Hz, 1H), 7.54 (s, 1H), 5.93 (s, 1H), 4.45 (s, 2H), 3.57 (s, 4H), 3.54 - 3.46 (m, 4H), 3.39 (g, J = 5.5 Hz, 2H), 3.22 (q, J = 5.8 Hz, 2H), 1.40 (s, 9H). ¹³C NMR (126 MHz, acetone- d_6) δ 167.4, 158.1, 156.7, 150.6, 140.7, 131.3, 78.7, 71.0, 70.8, 70.6, 70.2, 50.6, 41.0, 40.1, 28.6. ESI-MS, negative mode: m/z calcd mass for $C_{17}H_{27}FN_4O_7$ [M-H]⁻ = 417.1791, was found 418.00.

N-(2-(2-(2-aminoethoxy)ethoxy)ethyl)-2-(5-fluoro-2,6-dioxo-3,6-dihydropyrimidin-1(2H)-yl)acetamide TFA salt, 15: To a solution of compound 14 (94 mg, 0.224 mmol) in dry dichloromethane (2 mL), a solution of trifluoroacetic acid in dichloromethane (1 mL, 13.7 mmol in 1 mL) was added dropwise. The addition was performed under argon atmosphere at 0°C, and the reaction was stirred for 20 minutes at 0°C. The solvent evaporated under vacuum, and the residue was hexane/dichloromethane (1:1) and then with dichloromethane. After the washes, the resulting salt 15 (95 mg, 95%) was collected as a white solid and used in subsequent reactions without any further purification. 15: ESI-MS, positive mode: m/z calcd mass for $C_{12}H_{19}FN_4O_5$ [M+H]⁺ = 319.1412, was found 318.80.

2,2,2-trifluoro-N-(2-(2-(2-(2-(2-(2-(2-(10-10-2,6-dioxo-3,6-dihydropyrimidin-1(2H)-yl)acetamido)ethoxy)ethoxy)ethyl)acetamide, **17**: To a solution of compound **15** (95 mg, 0.22 mmol) in dry dimethylformamide (4.06 mL) and triethylamine (111 mg, 1.10

Open Access Article. Published on 29 September 2025. Downloaded on 10/26/2025 10:42:30 AM.

This article is licensed under a Creative Commons Attribution 3.0 Unported Licence

mmol), 4-nitrophenyl chloroformate (66.4 mg, 0.33 mmol) was added and the reaction was filtered under an argon atmosphere at 0°C, and the reaction was stirred for 3 hours at room temperature. The reaction mixture was filtered under vacuum and washed with ethyl acetate. The filtrate was concentrated under vacuum, and the residue was subjected to column chromatography (dichloromethane/methanol, isocratic elution 10:1) to obtain the carbamate analogue 239 (38 mg, 42%) as a white solid. **17**: ¹H NMR (500 MHz, acetone- d_6) δ 8.52 (s, 1H), 7.81 (d, J = 6.5 Hz, 1H), 7.56 (s, 1H), 4.44 (s, 2H), 3.64 – 3.60 (m, 2H), 3.60 – 3.55 (m, 4H), 3.54 – 3.49 (m, 4H), 3.43 – 3.37 (m, 2H). ESI-MS, positive mode: m/z calcd mass for $C_{14}H_{18}F_4N_4O_6$ [M+H]⁺ = 413.1090, was found 412.95.

N-(2-(2-(2-aminoethoxy)ethoxy)ethoyl)-2-(5-fluoro-2,6-dioxo-3,6-dihydropyrimidin-1(2H)-yl)acetamide hydrochloride, **18**: To a solution of compound **14** (36 mg, 0.086 mmol) in dry dioxane (0.39 mL), a solution of hydrochloric acid in dioxane (4 M, 1.55 mmol in 0.39 mL) was added dropwise. The addition was performed under an argon atmosphere at 0°C, and the reaction was stirred for 2 hours at 0°C. The solvent was evaporated under vacuum, and the resulting salt **18** (30 mg, 98%) was obtained as a white solid, which was used in subsequent reactions without any further purification. **18**: ESI-MS, positive mode: m/z calcd mass for $C_{12}H_{19}FN_4O_5$ [M+H]⁺ = 319.1412, was found 318.95.

4-nitrophenyl (2-(2-(2-(2-(5-fluoro-2,6-dioxo-3,6-dihydropyrimidin-1(2H)-yl)acetamido) ethoxy)ethoxy)ethyl)carbamate, **19**. To a solution of compound **18** (35 mg, 0.099 mmol) in dry dimethylformamide (1.5 mL) and DIPEA (38.3 mg, 0.296 mmol), 4-nitrophenyl chloroformate (26 mg, 0.128 mmol) was added and the reaction turns yellow in colour. The addition was performed under an argon atmosphere at 0 °C, and the reaction was stirred for 2 hours at room temperature. After complete consumption of the starting material, the solution containing the activated ester **19** was used directly in the next reaction without isolation. **19**: ESI-MS, positive mode: m/z calcd mass for $C_{19}H_{22}FN_5O_9$ [M+H]⁺ = 484.1474, was found 484.00.

(JH-VII-139-1)-(5-FU) conjugate, **geo140**: To a solution of JH-VII-139-1 (13 mg, 0.034 mmol), DIPEA (12 µL, 0.068 mmol) in dry dimethylformamide (0.75 mL), a crude solution of the activated ester 19 (1 equivalent) in dry dimethylformamide (0.75 mL) was added. The addition was performed under argon atmosphere, and the reaction was stirred for 24 hours at room temperature. After the complete consumption of JH-VII-139-1, the reaction was concentrated under vacuum, and the residue was subjected to column chromatography (ethyl acetate/methanol, gradient elution from 10:0.5 to 10:1) to obtain the final conjugate **geo140** (4.9 mg, 20%) as a green, fluorescent solid. **geo140:** ¹H NMR (500 MHz, DMSO- d_6) δ 8.45 – 8.41 (m, 2H), 8.35 (d, J = 8.1 Hz, 1H), 8.29 - 8.24 (m, 1H), 8.16 (s, 1H), 8.04 (s, 1H), 8.00 (d, J = 6.8 Hz,1H), 7.96 (s, 1H), 7.66 - 7.62 (m, 1H), 6.92 (d, J = 2.7 Hz, 1H), 5.42 (s, 1H), 4.26 (s, 2H), 3.61 - 3.45 (m, 8H), 3.43 - 3.38 (m, 2H), 3.24 - 3.19 (m, 2H), 2.93 (q, J = 7.5 Hz, 2H), 1.80 (s, 6H), 1.17 (t, J = 7.5 Hz, 3H). ¹³C NMR (126 MHz, DMSO- d_6) δ 179.0, 166.6, 162.3, 160.4, 157.6, 153.0, 149.7, 149.5, 145.5, 140.8, 139.3, 135.8, 135.5, 131.2, 129.7, 128.1, 127.7, 126.3, 126.1, 125.1, 121.7, 120.7, 116.6, 116.5, 109.4, 104.9, 69.6, 69.5, 69.0, 68.7, 49.6, 48.6, 48.5, 36.4, 29.9, 26.0, 15.2. ESI-MS, positive mode: m/z calcd mass for $C_{37}H_{37}FN_8O_7$ [M+H]⁺ = 725.2842, was found 724.85.

intestinalew Article Online DOI: 10:1039/D5MD00731C Biological experiments: Intestinal myofibroblast isolation: Primary subepithelial myofibroblasts were isolated from freshly collected intestinal mucosa biopsies as previously described, 28 from healthy individuals undergoing endoscopy for reasons of surveillance, after obtaining written and informed consent. Briefly, 4-6 pieces of intestinal tissue were collected in ice-cold Hank's Balanced Salt Solution (HBSS; Biosera, Nuaille, France) containing Ca²⁺/Mg²⁺ supplemented with P/S/A/G: Penicillin (100U/ml), Streptomycin (100μg/ml), Amphotericin (2.5 μg/ml) and gentamycin (50 µg/ml), followed by 15-minute washes with HBSS with and without Ca²⁺/Mg²⁺ to remove possible contaminants. Next tissue was de-epithelialized by a 15minute incubation in HBSS without Ca2+/Mg2+ containing 1mM Dithiothreitol (DTT, Sigma-Aldrich, Darmstadt, Germany) followed by 3x 30-minute washes in HBSS supplemented with 1mM ethylenediaminetetraacetic acid (EDTA, Sigma-Aldrich, Darmstadt, Germany) at 37 °C. Tissue was cultured in RPMI 1640 (PAN Biotech, Aidenbach, Germany) supplemented with 10% fetal bovine serum (FBS; Biosera, Nuaille, France) and P/S/A/G for as long as 30 days at 37 °C and 5% CO2. After colonies of myofibroblasts reached 30% confluency, cells were detached and consequently cultured in 75-cm² flasks in Dulbecco's Modifed Eagle Medium (DMEM, 4.5 g/l glucose; PAN Biotech, Aidenbach, Germany) with 10% fetal bovine serum and P/S/A.

Cell culture: HeLa, K562, HT-29, Caco-2, HepG2 and A549 cancer cell lines were obtained from the American Type Culture Collection (ATCC). All cell lines were cultured at 37 °C with 5% CO₂. HeLa, Caco-2, HepG2 and A549 cells were maintained in Dulbecco's Modified Eagle Medium (DMEM, PAN Biotech) supplemented with 10% FBS and antibiotics/antimycotics, while K562 cells were maintained in RPMI and HT-29 cells in McCoy's 5a medium (Biosera) with the same supplements.

Viability assays: All cells were seeded in 96-well plates (Corning, New York, USA) at density of 10⁴ cells per well, except HeLa that were seeded at destiny of 2x10³. After 24 hours, the cells were treated with increasing concentrations of the inhibitory compounds for 48 hours. Cytotoxic activity of parent and conjugate compounds was assessed by 3-(4,5-dimethylthiazol-2-yl)-2,5-diphenyltetrazolium bromide (MTT) assay, according to manufacturer's instructions. In brief, 100 μl of growth medium containing 0.5 mg/ml MTT (Sigma-Aldrich, Darmstadt, Germany) were added to each well of a 96-well plate and incubated at 37 °C and 5% CO₂ for 2 hours until the formation of visible intracellular purple crystals. Then, MTT-supplemented growth medium was discarded and 100μl dimethyl sulfoxide (Sigma-Aldrich, Darmstadt, Germany) were added per well for solubilization of dye. Absorbance was then measured on a microplate reader (Diareader EL 800; Dialab, Wr. Neudorf, Austria) at 570nm with a reference wavelength at 660nm.

In vitro kinase assays: Human SRPK1, SRPK2, and a turkey LBR N-terminal fragment (amino acids 62–92; LBRNt(62–92)) were expressed as GST-fusion proteins in bacteria using the pGEX-2T vector (Amersham Biosciences) as previously described. The GST-fusion proteins were purified with glutathione-sepharose resin (Amersham Biosciences) following the manufacturer's protocol. Kinase assays (25 μ L total volume) contained 0.5 μ g GST-SRPK1 or GST-SRPK2, 1 μ g GST-LBRNt(62–92) as substrate, 12 mM Hepes pH 7.5, 10 mM MgCl₂, 25 μ M ATP, and varying concentrations of inhibitors as indicated. Phosphorylated GST-LBRNt(62–92) was

detected by autoradiography (Super RX film, Fujifilm). Incorporated radioactivity was developed autoradioactivity was proposed proposed particle online quantified by scintillation counting of the excised SDS-PAGE gel bands.

Immunofluorescence: HeLa cells (3x10⁴ cells/well) were seeded on glass coverslips in 24-well plates. After 24 hours, cells were treated with the indicated concentrations of inhibitors for 24 or 48 hours. Following incubation, samples were fixed with 4% paraformaldehyde in PBS for 20 minutes at room temperature. Paraformaldehyde was quenched with 100 mM Tris-HCl (pH 7.5), and cells were permeabilized with 0.2% Triton X-100 in PBS for 10 minutes. Blocking was performed with 0.5% fish skin gelatin in PBS. Cells were then probed with a primary antibody (anti-SRPK1 monoclonal, 1:100 dilution, BD Biosciences, San Jose, CA, USA) and a secondary antibody (Alexa488-conjugated goat anti-mouse, 1:400 dilution, Molecular Probes, Eugene, OR, USA), followed by DNA staining with propidium iodide, as previously described.²⁵ Coverslips were mounted with mounting medium (0.01% *p*-phenylenediamine and 50% glycerol in PBS) and visualized using a Nikon confocal microscope with EZ-C1 3.20 software.

References

- 1. Zhou Z, Fu XD. Regulation of splicing by SR proteins and SR protein-specific kinases. Chromosoma 2013 Jun;122(3):191-207. doi: 10.1007/s00412-013-0407-z.
- 2. Nikolakaki E, Sigala I, Giannakouros T. Good cop, bad cop: The different roles of SRPKs. Front Genet. 2022 Jun 2;13:902718. doi: 10.3389/fgene.2022.902718.
- 3. Hogg EKJ, Findlay GM. Functions of SRPK, CLK and DYRK kinases in stem cells, development, and human developmental disorders. FEBS Lett. 2023 Oct;597(19):2375-2415. doi: 10.1002/1873-3468.14723.
- 4. Nikas IP, Themistocleous SC, Paschou SA, Tsamis KI, Ryu HS. Serine-Arginine Protein Kinase 1 (SRPK1) as a prognostic factor and potential therapeutic target in cancer: Current evidence and future perspectives. Cells 2019 Dec 19;9(1):19. doi: 10.3390/cells9010019.
- 5. Duggan WP, O'Connell E, Prehn JHM, Burke JP. Serine-Arginine Protein Kinase 1 (SRPK1): a systematic review of its multimodal role in oncogenesis. Mol Cell Biochem. 2022 Oct;477(10):2451-2467. doi: 10.1007/s11010-022-04456-7.
- 6. Bullock N, Oltean S. The many faces of SRPK1. J Pathol. 2017 Mar;241(4):437-440. doi: 10.1002/path.4846.
- 7. Nowak DG, Amin EM, Rennel ES, Hoareau-Aveilla C, Gammons M, Damodoran G, Hagiwara M, Harper SJ, Woolard J, Ladomery MR, Bates DO. Regulation of vascular endothelial growth factor (VEGF) splicing from pro-angiogenic to anti-angiogenic isoforms: a novel therapeutic strategy for angiogenesis. J Biol Chem. 2010 Feb 19;285(8):5532-40. doi: 10.1074/jbc.M109.074930.
- 8. Amin EM, Oltean S, Hua J, Gammons MV, Hamdollah-Zadeh M, Welsh GI, Cheung MK, Ni L, Kase S, Rennel ES, Symonds KE, Nowak DG, Royer-Pokora B, Saleem MA, Hagiwara M, Schumacher VA, Harper SJ, Hinton DR, Bates DO, Ladomery MR. WT1 mutants reveal SRPK1 to be a downstream angiogenesis target by altering VEGF splicing. Cancer Cell 2011 Dec 13;20(6):768-80. doi: 10.1016/j.ccr.2011.10.016
- 9. Wang P, Zhou Z, Hu A, Ponte de Albuquerque C, Zhou Y, Hong L, Sierecki E, Ajiro M, Kruhlak M, Harris C, Guan KL, Zheng ZM, Newton AC, Sun P, Zhou H, Fu XD. Both decreased and increased SRPK1 levels promote cancer by interfering with PHLPP-mediated

- dephosphorylation of Akt. Mol Cell 2014 May 8;54(3):378-91 doj Kew Article Online 10.1016/j.molcel.2014.03.007.
- 10. Fukuhara T, Hosoya T, Shimizu S, Sumi K, Oshiro T, Yoshinaka Y, Suzuki M, Yamamoto N, Herzenberg LA, Herzenberg LA, Hagiwara M. Utilization of host SR protein kinases and RNA-splicing machinery during viral replication. Proc Natl Acad Sci U S A. 2006 Jul 25;103(30):11329-33. doi: 10.1073/pnas.0604616103
- 11. Batson J, Toop HD, Redondo C, Babaei-Jadidi R, Chaikuad A, Wearmouth SF, Gibbons B, Allen C, Tallant C, Zhang J, Du C, Hancox JC, Hawtrey T, Da Rocha J, Griffith R, Knapp S, Bates DO, Morris JC. Development of potent, selective SRPK1 inhibitors as potential topical therapeutics for neovascular eye disease. ACS Chem Biol. 2017 Mar 17;12(3):825-832. doi: 10.1021/acschembio.6b01048.
- 12. Hatcher JM, Wu G, Zeng C, Zhu J, Meng F, Patel S, Wang W, Ficarro SB, Leggett AL, Powell CE, Marto JA, Zhang K, Ki Ngo JC, Fu XD, Zhang T, Gray NS. SRPKIN-1: A covalent SRPK1/2 inhibitor that potently converts VEGF from pro-angiogenic to anti-angiogenic isoform. Cell Chem Biol. 2018 Apr 19;25(4):460-470.e6. doi: 10.1016/j.chembiol.2018.01.013.
- 13. Thysiadis S, Katsamakas S, Dalezis P, Chatzisideri T, Trafalis D, Sarli V. Novel c(RGDyK)-based conjugates of POPAM and 5-fluorouracil for integrin-targeted cancer therapy. Future Med Chem. 2017 Dec;9(18):2181-2196. doi: 10.4155/fmc-2017-0139
- 14. Chatzisideri T, Leonidis G, Sarli V. Cancer-targeted delivery systems based on peptides. Future Med Chem. 2018 Sep 1;10(18):2201-2226. doi: 10.4155/fmc-2018-0174.
- 15. Leonidis G, Dalezis P, Trafalis D, Beis D, Giardoglou P, Koukiali A, Sigala I, Nikolakaki E, Sarli V. Synthesis and Biological Evaluation of a c(RGDyK) Peptide Conjugate of SRPIN803. ACS Omega 2021 Oct 14;6(42):28379-28393. doi: 10.1021/acsomega.1c04576.
- 16. Leonidis G., Koukiali A., Sigala I., Tsimaratou K., Beis D., Giannakouros T., Nikolakaki E., Sarli V. Synthesis and anti-angiogenic activity of novel c(RGDyK) peptide-based JH-VII-139-1 conjugates. Pharmaceutics 2023, 15(2):381. doi: 10.3390/pharmaceutics15020381
- 17. Greenwald, R. B.; Pendri, A.; Conover, C. D.; Zhao, H.; Choe, Y. H.; Martinez, A.; Shum, K.; Guan, S. Drug delivery systems employing 1,4- or 1,6-elimination: poly(ethylene glycol) prodrugs of amine-containing compounds. *J Med Chem.* **1999**, 42, 3657-3667. DOI: 10.1021/jm990166e.
- 18. Jeffrey, S. C.; Torgov, M. Y.; Andreyka, J. B.; Boddington, L.; Cerveny, C. G.; Denny, W. A.; Gordon, K. A.; Gustin, D.; Haugen, J.; Kline, T.; Nguyen, M. T.; Senter, P. D. Design, synthesis, and in vitro evaluation of dipeptide-based antibody minor groove binder conjugates. *J Med Chem.* **2005**, 48, 1344-1358. DOI: 10.1021/jm040137q.
- 19. Chatzisideri T, Leonidis G, Karampelas T, Skavatsou E, Velentza-Almpani A, Bianchini F, Tamvakopoulos C, Sarli V. Integrin-Mediated Targeted Cancer Therapy Using c(RGDyK)-Based Conjugates of Gemcitabine. J Med Chem. 2022 Jan 13;65(1):271-284.
- 20. Voukkalis N., Koutroumani M., Zarkadas C., Nikolakaki E., Vlassi M., Giannakouros T. SRPK1 and Akt Protein Kinases phosphorylate the RS domain of Lamin B Receptor with distinct specificity: A combined biochemical and In silico approach. PLoS One 2016, 11(4):e0154198. doi: 10.1371/journal.pone.0154198.
- 21. Zhong X.Y., Ding J.H., Adams J.A., Ghosh G., Fu X.D. Regulation of SR protein phosphorylation and alternative splicing by modulating kinetic interactions of SRPK1 with molecular chaperones. Genes Dev. 2009, 23:482–495. doi: 10.1101/gad.1752109.
- 22. Edmond V., Moysan E., Khochbin S., Matthias P., Brambilla C., Brambilla E., Gazzeri S., Eymin B. Acetylation and phosphorylation of SRSF2 control cell fate decision in response to cisplatin. EMBO J. 2011, 30:510–523. doi: 10.1038/emboj.2010.333.

- 23. Vivarelli S., Lenzken S.C., Ruepp M.D., Ranzini F., Maffioletti A., Alvarez R., Mühlemanne Article Online O., Barabino S.M. Paraquat modulates alternative pre-mRNA splicing by modifying the intracellular distribution of SRPK2. PLoS One 2013, 8:e61980. doi: 10.1371/journal.pone.0061980.
- 24. Sigala I., Koutroumani M., Koukiali A., Giannakouros T., Nikolakaki E. Nuclear translocation of SRPKs Is associated with 5-FU and cisplatin sensitivity in HeLa and T24 cells. Cells 2021, 10(4):759. doi: 10.3390/cells10040759.
- 25. Voskuhl, J.; Waller, M.; Bandaru, S.; Tkachenko, B. A.; Fregonese, C.; Wibbeling, B.; Schreiner, P. R.; Ravoo, B. J. Nanodiamonds in sugar rings: An experimental and theoretical investigation of cyclodextrin-nanodiamond inclusion complexes. *Org. Biomol. Chem.* **2012**, 10, 4524-4530. DOI: 10.1039/C2OB06915F.
- 26. Vong, K. K.; Maeda, S.; Tanaka, K. Propargyl-Assisted Selective Amidation Applied in Cterminal Glycine Peptide Conjugation. *Chemistry.* **2016**, 22, 18865-18872. DOI: 10.1002/chem.201604247.
- 27. Yue, K.; Hou, X.; Jia, G.; Zhang, L.; Zhang, J.; Tan, L.; Wang, X.; Zhang, Z.; Li, P.; Xu, W.; Li, X.; Jiang, Y. Design, synthesis and biological evaluation of hybrid of ubenimex-fluorouracil for hepatocellular carcinoma therapy. *Bioorg Chem.* **2021**, 116, 105343. DOI: 10.1016/j.bioorg.2021.105343.
- 28. Filidou, E.; Valatas, V.; Drygiannakis, I.; Arvanitidis, K.; Vradelis, S.; Kouklakis, G.; Kolios, G.; Bamias, G. Cytokine Receptor Profiling in Human Colonic Subepithelial Myofibroblasts: A Differential Effect of Th Polarization–Associated Cytokines in Intestinal Fibrosis. *Inflamm. Bowel Dis.* **2018**, *24*, 2224–2241. https://doi.org/10.1093/ibd/izy204

The data supporting this article are available in its ESI. The ESI contains copies of Double Online and 13C NMR spectra, 2D NMR spectra, MS spectra, and analytical HPLC traces for all final compounds.